Differentiation of cortical areas: effects of free energy minimization with broken symmetry.

James Wright [1] and Paul Bourke [1]

[1] Centre for Brain Research, School of Medicine, University of Auckland, Auckland, New Zealand.

Corresponding author JJ Wright.

Phone +64 9 4835024 or +64 21 955017

Email jj.w@xtra.co.nz

Abstract

We studied separation and integration of cortical areas during cortical neurogenesis, using growth simulations that depend upon matching of spatial frequencies between areas – a method equivalent to maximizing zero-lag pulse synchrony and minimizing prediction errors. In a uniform neural field, areas would emerge as mirror pairs with intervening Markov blankets, but regional disparities break this mirror symmetry. Differential effects of disparity of information inputs, cell types, and axonal lengths were characterised in the simulations, explaining how asymmetries of information transfer arise and lead to greater or lesser segregation of systems, sequencing of exchanges, and reciprocal control effects. In the developmentally completed form, nonspecific excitation and frequency modulation from limbic and subcortical sources would modulate exchanges and sequencing, introducing non-hierarchical information flows within the hierarchical radial architecture.

1. Introduction

The differentiation of the cerebral cortex into cellularly distinct areas with segregation and integration of function has long been recognised (Brodmann 1909, Yeo et al. 2011, Zeki and

Shipp 1988). In this paper we set out some findings relevant to the interaction and differentiation of cortical areas, aiming to further dissect the way in which epigenetic prescription of cell characteristics, apoptotic selection, and neural dynamics are intertwined.

Our account draws upon the Free Energy Principle of Friston and colleagues (Friston 2002, 2005, 2010, Hohwy 2016, Friston et al. 2017, 2022, Buckley et al. 2017, Kirchoff et al 2018), the Structural Model of Barbas et al. (Barbas 1986, 2015, Barbas and Rempel-Clower, 1997) and related work (Sanides 1962, 1964, 1970, Garcia-Cabezas et al. 2014, 2019, 2017, 2020, Rakic 2002, Puelles et al. 2019, 2024, Sancha-Velasco et al. 2023), and the functional interpretation of radial neocortical organization of Tucker and colleagues (Tucker and Luu 2021, 2023, Luu et al. 2024).

A motivation for the work was to establish a more general account of non-hierarchical cortical interactions, within established models of hierarchical order. Our agenda — in this and previous work — is to understand the principles that underlie cortical neurogenesis and the means by which a world model emerges, able to undertake subsequent inference and learning. In this paper we particularly want to consider how architectures of both radial and lateral (i.e., circumferential) connectivity emerge and interact. We will use simulations that are founded in biologically specific neurodynamical and anatomical/geometric terms. The basic arguments can be read as special instances of general abstract dynamical concepts of statistical dynamics, active inference, generalised synchrony, Markov boundaries, and their relationship to free energy. Boxes 1,2, and 3 provide a description of these background technical concepts.

Turning to the embryological context - as recently summarized in Luu et al (2026), beginning from spinal segments with dorsal-ventral organization described by the prosomeric model (Nieuwenhuys 2011), and under the influence of trophic factors, at the rostral extension of the alar plate and the level of the hypothalamus the dorsal-ventral organization gives way to the rostro-caudal order of the structural model. Separate radiations from hypothalamic and olfactory origins will become the dorsal and the ventral neocortices. Via the alar plate, these extensions arise from the spinal somato-sensory and viscero-sensory dorsal component of the spinal system, the more ventral, and therefore visceral, component becomes extended via rostral projections in layers 5,6 and 2,3, of the developing neocortex, while the more dorsal, somatic component extends outward in layer 4. This rostro-caudal order develops in both neocortical divisions, and within each a counterflow develops in which, from more rostral origins, including primary sensory and motor cortices, signals passing along layer 4, encounter signals of caudal origin in layers 5,6 and 2,3, and interact at the 3,4 boundary. The greater thickness in layer 4 (Barbas and Garcia-Cabezas 2015, 2016) in ventral neocortex biases the ventral neocortex toward limbi-petal flow, and vice-versa for dorsal neocortex - with attendant neurone tuning to movement recognition and modulation of control in the dorsal system, versus ventral neocortex emphasis on object recognition and recall (Trevarthan 1968, Ungerleider and Mishkin 1982, Yang et al. 2022). These developments impose a fundamental hierarchical order upon the neocortex.

Tucker and Luu argue the sources of the dorsal and ventral neocortical divisions served elementary “go” versus “stop” roles at the most primitive stage of encephalization, and that this functional distinction still underlies the dorsal division’s initiation of actions and control

of internally directed attention and implicit memory, versus the ventral division's association with alerting responses to novel sensory material and recall of explicit memories. The divisions are served by separate thalamic relations (Cisek 2022, Butler 2008), and separate cortical activation systems – the lemnothalamic activation system serving the dorsal division and the collothalamic system the ventral division (Butler 2008, Loonen and Ivanova 2016) - the dorsal system noradrenergic, serotoninergic and acetylcholinergic; the ventral dopaminergic. (Hansen et al 2022, Froudist-Walsh 2023). The divisions differentially mediate rapid eye movement (REM) sleep, and slow-wave sleep (SWS) (Tucker et al, 2025). The lemnothalamic inputs drive cortical desynchronization and release capacity for impulsion of overt behaviour, and the collothalamic activates the ventral division during response to novelty (Stenberg 2007).

In Tucker et al.'s accounts the radial order of the cortex provides for both Active Inference and Active affordance – concepts central to the Free Energy Principle. By active inference (as discussed in context throughout the paper) a generative model of the self-in-the-world arises, while active affordance – generated by inputs from lower limbic components imposing phylogenetically determined values – guides active inference along most survival-beneficial pathways. Providing a mechanism of active inference, they draw upon a widely applied model of predictive error minimization (Bastos et al. 2012, 2020, Adams et al. 2013, Shipp and Friston 2022,) which lays emphasis upon excitatory/inhibitory cancellations in the counterflow contacts at levels 2,3 with 4. Active affordance is attributed to more complicated interactions with subcortical systems (Luu et al. 2026), partly dopamine mediated (Friston et al. 2012)

The above strictly radial account minimizes the role of circumferential cortico-cortical connections. Along the radial lines of development circumferential connections form between all cortical layers - so that overall connectivity comes to conform to the distance rule – that is, mean distances of connection between individual neurons and cortical areas are minimized toward a small-world optimum (Markov et al. 2011, Vezoli et al. 2021, Aparicio-Rodriguez and Garcia-Cabezas 2023). The contrast of radial versus circumferential connectivity raises considerations of hierarchical versus non-hierarchical information processing. Were prediction errors minimized in strictly hierarchical order along the radial lines, it has been argued that they would be logically restricted (Kwisthout and van Rooji 2020). A simple hierarchical (radial) architecture is not sufficient to account for segregation or factorisation within any given level, and circumferential (lateral) interactions may be necessary for logical generality, in the way that a computer program requires conditional "go-to" instructions as well as step-by-step sequences. We will suggest means whereby hierarchical and non-hierarchical processes of association and error minimization can take place.

Circumferential intracortical and cortico-cortical connections introduce a great deal of further complexity to the neocortical order. Brodmann areas and Yeo areas highlight diversity in cell types and axonal lengths. These diverse areas form systems of distributed functional networks. Yeo et al (2011) cite Goldman-Rakic (1988), who offered three specific anatomical observations that provide evidence for distributed functional grouping in networks. Firstly, prefrontal and parietal areas that are directly connected to one another also tend to have convergent projections to additional temporal and limbic areas. Secondly, interconnected association areas are tied together by common thalamic connections, and

thirdly, interconnected association areas tend not to have laminar projection patterns with clear feedforward and feedback relations, as seen in the radial order of the structural model. Association cortex is characterized by multiple highly interconnected modules (Basset and Bullmore 2006) each made up of nodes distributed widely across the cortex, and formed largely of circumferential rather than radial structures. These form functionally separable sub-systems – as examples, the default mode and semantic networks (Thye et al. 2025), and the separation of functions of left and right hemispheres (Sperry 1981).

In earlier work, and against the background of all of the above, we have proposed a theory of self-organisation in the developing neocortex, in which selection during neurogenesis of neurone assemblies that maximize synchrony and ultra-small world organization (Heck et al 2008, Downes et al 2012, Holville et al 2019, Perin et al. 2011, Sang et al. 2021) leads to neural networks emerging in mirror-symmetric patterns, forming 1:1 maps at multiple scales. The theory was developed initially in regard to contextual connections at mesoscale in cortical layers 2,3, and extended to development of connections within the structural model. It is complementary to, but distinct from, feedforward concepts that emphasise feature detections. Crucially, it explains how during embryogenesis connections form 1:1 maps enabling storage of images consistent with the topology of space and time, so that, postnatally, spatiotemporal images can be read in and out of cortical networks , sensory impressions stored and associated, and expressed in patterns of motor activity. This model implies prediction error minimization is ubiquitous at all scales and levels of interaction. Details are given in Wright and Bourke (2024a,b, 2025) and in the Appendix.

While approximation to mirror symmetry between cortical areas is apparent, for instance in the interlinkages of cortical visual areas (Wandell et al. 2007) and in the auditory system (Formisano et al. 2003), no cortical or cerebral areas are perfectly mirror symmetric. We will show how asymmetries short of the idealized mirror symmetries can give rise to cortical area specializations and sequential ordering of information processing in both hierarchical, and non-hierarchical, manners, and subject to interaction with limbic and activation systems. We begin by reviewing our previous account as necessary background to the presently reported simulations.

2. Self-organization in the developing neural field.

Assumptions made about the neural field have been kept as simple as possible, so neural field equations are in minimal and general form.

2.1 Presynaptic flux and Hebbian plasticity

Unidirectional flows of presynaptic flux in a neural field can be represented as n elements of a square matrix $\Phi(t)$, with elements φ_{ij}, the pre-synaptic flux received at the neuron at position i from the neuron at position j, over all pathways.

$$\Phi(t) = GQ(t) \qquad 1$$

$G(t)$ is a square matrix operator of presynaptic gains and axo-dendritic conduction times, transforming $Q(t)$, a vector of action potential pulse rates of all neurons, so that

$$\varphi_{ij}\left(t+\frac{|i-j|}{\nu}\right)=\varepsilon_{ij}g_{ij}\rho_{ij}Q_j(t) \qquad 2$$

Q_j is the pulse rate of the $j-th$ neuron, υ is the speed of signal spread, and $\frac{|i-j|}{\nu}$ is the delay from pulse generation to arrival of peak pulse density at pre-synapses on the $i-th$ neuron, averaged over all routes. Synaptic gains are on three time-scales, $\varepsilon_{ij}, g_{ij}, \rho_{ij}$ - the transient synaptic efficacy, the slow dynamic synaptic gain, and the structural synapse gains respectively, with synaptic flux either excitatory or inhibitory. Gains are competitive on all three time-scales (Miller 1996, Okomoto and Ichikawa 2000) and consistent with unification of fast and slow synaptic learning rules (Izhikevich and Desai 2003). Thus, with ongoing network activity the rapid and transient synaptic efficacies in response to afferent pulses lead to increasing dynamic and structural gains as the time average of synaptic flux.

2.2 Dendritic summation and pulse generation

Transformations of synaptic flux leading to pulse generation are

$$V_i(t)=\delta(t-\tau)*\sum\varphi_{ij}\,(t) \qquad 3$$

where $\delta(t-\tau)$ is a dendritic delay function convolving the aggregate presynaptic flux to generate the dendritic potential, $V_i(t)$, and

$$Q_i(t)=f_\theta\big(V_i(t)\big) \qquad 4$$

$Q_i(t)$ is the efferent pulse rate of the $i-th$ neuron, and f_θ is any sigmoid-like function operating as a probabilistic threshold for action potential generation,

2.3 Anti-Hebbian plasticity and steady state

Anti-Hebbian synaptic plasticity, reflecting multiple homeostatic metabolic pathways, acts to normalise excitatory and inhibitory synaptic gains, leaving the relative strengths of Hebbian influences unchanged (Keck et al 2017). In steady state of individual neurons, and the population average, if $\sum \varphi_e$ is the total excitatory presynaptic flux and $\sum \varphi_i$ is the total inhibitory presynaptic flux, then

$$\sum \Phi_{\mathrm{e}} \rightarrow \sum \varphi_{\mathrm{i}} \rightarrow \text{constancy} \qquad 5$$

The steady-state level may be varied by the level of activation of the network.

2.4 Mechanism of synchrony, and elementary prediction error minimization

Synchronous oscillatory firing (Singer 1993) of cortical neurones is prominent in the 40 Hz (gamma) range but is apparent over all frequencies. Synchrony emerges in any network with zero-mean summing junctions interposed between elements, even when the network is driven by temporally and spatially diffuse white noise (Chapman et al 2002, Wright et al 2000). Principal component spatial eigenmode analysis of simulations of the neural field show that the first principal component of the field is widespread zero-lag synchrony with relatively low spatial damping, and is the response to the even components of the inputs driving the field. The second principal component is low magnitude, asynchronous, highly

spatially damped, rapidly dissipated activity, and is the response to the odd components of the inputs. Closely related simulations accounting for the background EEG spectrum and major cerebral rhythms (Wright and Liley 1995, 1996, Robinson et al 1997, 2001, Rennie et al 2000, 2002) include prominent zero lag synchrony as an inherent property.

Generation of the principal components can be explained as follows. Oscillation arises from the to-and-fro exchange of signals between excitatory neurons and local inhibitory neurons. Synchrony is then generated by summation of synaptic afferents at dendritic membranes, as in equation (3), with an adjusted set level as in equation (5). Synaptic pulse trains that arrive in opposite phase with respect to the sustained mean level cancel in summation, while those in phase summate positively – thus out-of-phase signals are dissipated, whereas in-phase pulses, exchanged through the neural population, converge to coordinated synchrony at all frequencies. This applies to the summation of both excitatory and inhibitory synaptic fluxes, since inhibitory flux is effectively of reverse phase to excitatory flux. The argument is independent of details of the statistics of pulse generation and exchange, since only interactions of odd and even signal components are of relevance.

Figure 1 left shows the way in which the collision of odd (antiphase) and even (in phase) signals electrocortical waves results in their mutual dissipation or additive reinforcement respectively. Thus the exchange of signals between any two neurons will tend to converge toward their synchronous firing, providing a prototypical form of predictive error minimization and maximization of mutual information, I. Roughly measured in linear approximation,

$$I = -\frac{1}{2} log_2(1 - r^2) \qquad 6$$

where r is the correlation coefficient of their synaptic flux exchange. From this simple form of prediction error minimization between individual cells the formation of geometrically ordered multi-way exchanges between cell populations can arise as described in the next sections.

Box 1: synchrony and self-organisation

Sparsely coupled dynamical systems occur widely in many physical systems including neural networks and coupled map lattices (Breakspear 2002, Breakspear and Stam 2005, Ito and Kaneko 2000, Lungarella and Sporns 2006, Pyragas 1997). In these systems asymmetries in coupling preclude the system from settling into an equilibrium, so that they remain in nonequilibrium steady-state (Jarzynski 1997, Jiang et al. 2004, Kwon and Ao 2011, Nicolis and Prigogine, 1977) and the trajectories of their motion have characteristic itinerancy, which may or may not be chaotic (Namikawa 2005, Nara,2003;,Tsuda, 2001). Such systems can be characterised by a Lyapunov function that decreases monotonically as the system evolves to its nonequilibrium steady state. The Lyapunov function can be interpreted as difference of variational free energy between the current probabilistic configuration and the final (steady-state) probability density, expressed in terms of a relative entropy, or KL divergence (a measure of statistical distance) between the current density and steady-state density (Pavlos et al. 2012, Yuan et al. 2010).

A second characterisation of self-organisation in the wider sense is in terms of generalised synchrony (a.k.a., synchronisation of chaos)(Jafri et al. 2016, Schiff et al. 1996, Schumacher et al. 2012). This usually rests upon a partition of the system into two or more parts that are loosely coupled, as may be seen for example in turbulent flows. Generalised synchrony occurs when the dynamics start to synchronise across their joint space (Breakspear 2004), and generalised synchrony is the nonequilibrium steady-state solution that minimises free energy. In the special case that the two parts the system are structurally symmetric, then the ensuing synchrony is called identical synchronisation. Our treatment of anatomical organization in mirror pairs, with dynamical stable or unstable fixed points at or near a minimum of free energy, is thus a simplified description of a system in nonequilibrium steady-state that approaches identical synchronisation.

2.5 Gamma oscillation, wave interactions and period doubling

In simulations with physiologically appropriate parameters a primary frequency of oscillation arises in the gamma range, with a period $\frac{1}{\gamma} = \frac{2|i-j|}{v}$, where $|i-j|$ is the distance of separation of closely situated excitatory and inhibitory neurones in layers 2,3, and γ is the gamma frequency. When phase aligned, additive wave interactions can then occur at periods $\frac{m}{\gamma}$ $(m = 1, 2,3,4..)$. On a pathway to generation of a $\frac{1}{f}$ power spectrum, further summations at periods $2m = 2,4,6,8..$ create period doubling at frequencies $\gamma/2$, $\gamma/4$, $\gamma/8$ .. - frequencies close to the beta, alpha, and theta frequencies. When the neural field receives inputs at these frequencies, additive and dissipative wave interactions will result in co-resonances with phase alignments matched to the inputs. This suggests a

means by which the cortical neural field might interact with, or be controlled by, rhythmic inputs.

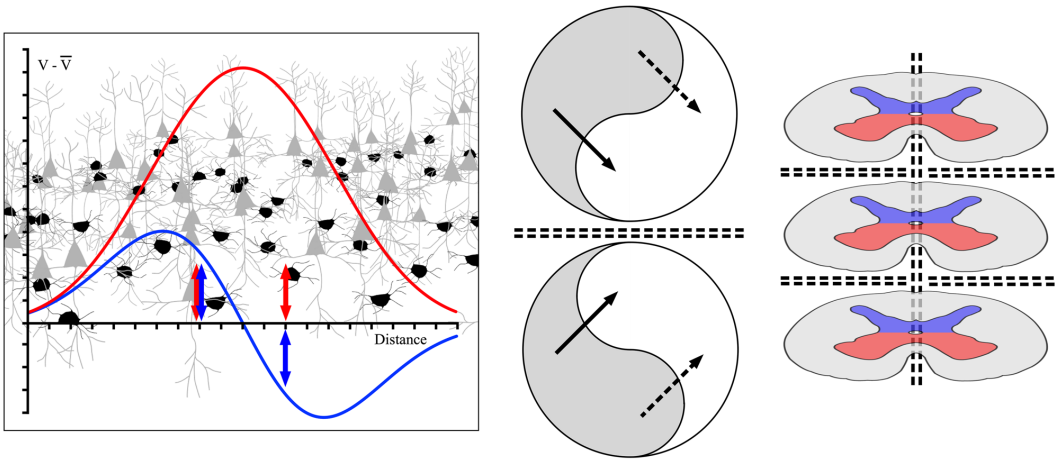

Figure 1.

Left. Mean field origin of synchrony among sparsely connected excitatory (grey) and inhibitory (black) neurons. Local field potential ($V - \bar{V}$) versus distance of separation. In-phase pulses (red arrows) generate synaptic summations at dendritic membranes shown by red curve. Out of phase pulses (blue arrows) dissipate at membranes (blue curve).

Middle: Mirror paired neural systems with coupled spatial eigenmodes (arbitrary grey and white yin-yang figures) generate travelling waves that cancel about the line of reflection (dashed black lines) creating a Markov blanket.

Right: Putative Markov blankets in spinal cord, between axes of bilateral symmetry, and between mirror-symmetric spinal segments.

2.6 The generation of mirror-paired networks in the neural field

2.6.1 Minimization of variational free energy.

Hebbian learning leads to a fall in the variational free energy of presynaptic flux, F, as cross-connections form.

$$F = A - C \to 0 \qquad 7$$

where A is total presynaptic flux autocorrelation, and C is total presynaptic flux cross-correlation. At the limit $F \to 0$, for all synaptic fluxes φ_{ij} and φ_{ji}, exchanged with time-lag τ, the sum of their autocorrelations is equal to the sum of their cross-correlations - ie:

$$\varphi_{ij}(t)\varphi_{ij}(t-\tau) + \varphi_{ji}(t)\varphi_{ji}(t-\tau) = \varphi_{ij}(t)\varphi_{ji}(t-\tau) + \varphi_{ji}(t)\varphi_{ij}(t-\tau) \qquad 8$$

According to the free energy principle the synaptic fluxes now represent the spatial and temporal associations in the network's inputs. (see Box 3.)

Equilibrium requires that energy approach equipartition: $\varphi_{ij}(t) \to \varphi_{ij}(t-\tau) \to \varphi_{ji}(t) \to \varphi_{ji}(t-\tau)$. The equilibrium condition is met when pairs of excitatory cells, or pairs of inhibitory cells, exchange equal and opposite flux at zero lag ($\tau = 0$), and when pairs of cells, one inhibitory the other excitatory, exchange flux by firing in opposite phases of the gamma rhythm cycle, with lag $\tau = \frac{|i-j|}{v}$. Thus the equilibrium state is synchronous oscillation. Consequently a ground state of universal synchrony is continuously approached at all time scales in the developing network, and synaptic consolidation proceeds to maximize synchrony to the degree possible in the face of external perturbations.

Close approach to minimum free energy implies a large information storage capacity, even if individual synaptic connections are merely binary valued. From Nyquist and Shannon theorems, the information storage capacity, D, for n synapses, is given by

$$D = nlog_2\left(1 + \frac{C}{A}\right) \quad 9$$

So as $C \to A$, $D \to n$. Large storage capacity at all stages of development implies that early simple learning can take place with high degeneracy, and later differentiation.

2.6.2 Prediction error minimization, free energy gradient, and excitatory-inhibitory balance

Solutions to equation (8) in which free energy is zero but energy is not equipartitioned, represent forces perturbing the system - external inputs operating upon the neural network – and are analogous to pdV forces in equilibrium thermodynamics, where free energy is Gibbs free energy. As connections consolidate, fields of synchrony form spatial eigenmodes of the network, and asymmetric couplings store information on time variations in input signals, so the whole becomes a system of coupled spatial eigenmodes.

Free energy gradients must vanish as the free energy is minimised - but since the system is under continuing input perturbations, then, where $\Delta\Phi^+$ is a vector representing flux induced by the externally imposed signals, there must arise an oppositely directed vector $\Delta\Phi^-$; in effect the neural network predicting and neutralizing its inputs with minimal error.

Opposite and equal compensating asymmetric exchanges cannot be within the same eigenmode system, as this would result in a frozen steady state in which representation of input time-variations would not be possible. Therefore spatial eigenmodes must develop in paired systems with mirror reversal, each of a pair with time-varying flux exchanges between eigenmodes oppositely directed to those in the mirror partner.

The paired mirror systems must maintain overall excitatory/inhibitory balance, as required by equation (5). This can be provided at the line of interaction of the mirror pair by anti-Hebbian plasticity of all excitatory and inhibitory couplings. The line of collision acts as a Markov blanket (Friston, 2002,2008, 2010, 2022, Friston and Ao 2012, Friston and Buzsaki 2016, Friston et al. 2017, 2020, 2021, Palacios et al 2020, Parr et al 2022, Ramstead et al. 2022) – that is, any boundary, or manifold, over which exchanges between two systems converge to maximum synchrony, minimum free energy, and minimized prediction errors.

Box 2: boundaries and Markov blankets

The separation of a dynamical system into two or more parts rests on being able to draw a boundary that separates one part from another. Under the free energy principle this boundary corresponds to a Markov blanket (Pearl 2009); namely, a set of states that renders dynamics internal to the boundary conditionally dependent of states that are external.

Markov blankets emerge in two settings in the current work, because in terms of the radial (hierarchical) structure, Markov blankets define the statistical separation of both cortical layers and hierarchical levels in a hierarchy (i.e., under the structural model).

Technically, a Markov blanket of a neurone or neuronal population is defined by its parents (i.e., afferents) children (i.e., efferents) and the parents of children. For example, in the radial architecture of inter-and intra-laminar connections (see Figure 2a) we can identify the Markov blanket of granular layer 4 as follows: its parents are the superficial layers (2 and 3) of the hierarchical level below and the deep layers (5 and 6) of the level in question. Its children and the superficial layers of the current level and the parents of its children are the deep layers of the level above. So the ensuing Markov blanket defines both a laminar partition — within cortical layers — and a hierarchical level in terms of any level's neighbours. Similar arguments can be made for the lateral or circumferential connections that afford a midline Markov blanket in the context of mirror symmetry (see Figure 2b). This implies a multiplicity of Markov blankets partitioning neuronal states or populations at the laminar, intra-areal and inter-areal levels. In the preceding work of Wright and Bourke the existence of embedded layers of Markov blankets was inferred from the anatomical configurations that arise as synchronous oscillation is maximized during neurogenesis.

A Markov blanket of this type need not be a static cancellation barrier. It is a line of exchange that by fluctuation, transmits signals between the paired systems, so the paired structure conforms to the good regulator theorem (Conant and Ashby 1970), meaning that each of the paired systems acts to minimize prediction errors in exchange with the other. This is a specific instance of the emergence of generalized synchrony (see Box 1, and for an example of the wide applicability of the generalized form, see Friston and Frith, 2015.) Multiway exchanges between many interlinked mirror pairs can then form a self-regulating

adaptive system, in which perturbations of exchanges over the Markov blankets act to coordinate interactions over wide ranges.

Figure 1 middle shows the topology of an idealized mirror pair system with intervening Markov blanket, and Figure 1 right shows that the structure of the spinal cord can be regarded as an approximation to mirror pairs created by bilateral symmetry, and by segmental symmetry (Wright and Bourke 2025).

2.7 Formation of mirror pairs during embryogenesis

Figure 2(a) shows schematically the way that the emergence of mirror pairs can occur between the counterflows of signals in the radial lines of neurodevelopment described in the Structural Model, indicating the points of contact between layers 2,3 and 4, at which preliminary formation of Markov blankets can occur, paving the way for integration of function between limbic and primary neocortical areas.

Figure 2(b) shows how the concurrent circumferential development of connections favours bidirectional exchanges between cortical areas and thus mirror pairing between cortical areas. This figure is also intended to suggest mirror systems at mesoscale can arise as columnar and superficial patch systems, breaking the cortex into a multitude of modules with greater overall stability (see Appendix).

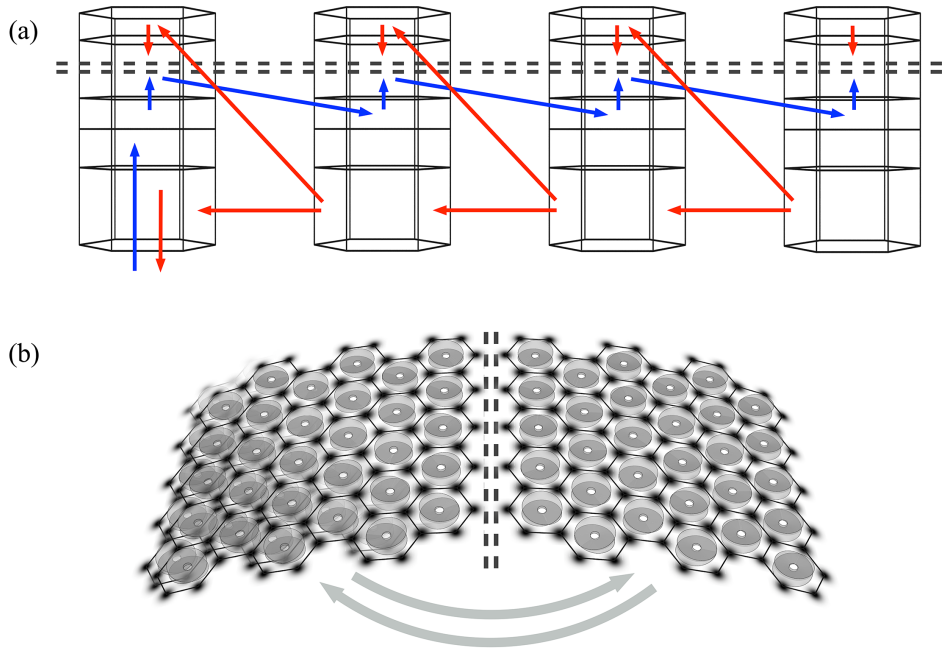

Figure 2.

(a) Signal flows in the radial lines of the Structural model. Blue arrows – synaptic flux in layer 4. Red arrows – synaptic flux in layers 5,6 and 2,3. Markov blankets form at the 2,3 versus 4 junction.

(b) Formation of circumferential interareal connections. Cortical areas bilaterally coupled by cortico-cortical fibres (grey arrows) link multi-columnar systems within each area.

Box 3: Markov blankets and active inference

An important implication of a Markov blanket is that one can apply the free energy principle and interpret the dynamics internal to a boundary as, effectively, inferring states that are external to the boundary; namely, active inference. This follows from the physics of self-organisation under Markov blankets (Friston et al. 2023), in which internal dynamics follow a gradient flow of variational free energy, and can be read as a bound on the surprisal (a.k.a., self-information) of exchanges across the Markov blanket. One

commonly applied formulation of the implicit (Bayesian) mechanics is predictive coding, in which the superficial layers encode prediction errors, while deep layers encode representations that provide predictions for lower levels (Bastos et al. 2012). Prediction errors — that report surprisal — are, mathematically, equivalent to free energy gradients, (Sengupta et al. 2013) so as the variational free energy is minimised surprisal vanishes. This means that self-organisation arises as prediction errors are minimized and generalised synchrony is approached at a nonequilibrium steady-state (See Box 1). The gradients (i.e., prediction errors) will never attain zero, and will evince divergence-free, oscillatory dynamics.

Our argument presents the case that elementary properties of the neural field and disparities in cell types and architecture impose conditions for the emergence of a non-equilibrium steady state, with Markov blankets and capacity for active inference.

3. The impact of asymmetries.

3.1 Asymmetry and unstable fixed points

In an idealised and isolated mirror pair, perfect stable equilibrium would be attained – ie:

$$\Delta\Phi^{+}(t) - \Delta\Phi^{-}(t) \to 0\,, \frac{dF}{dt} \to 0, and\ \frac{d^2F}{dt^2} \to 0 \qquad 10$$

When two imperfectly matched neural systems approach stable exchange over their intervening blanket, all three of the conditions in equation (10) cannot be attained. Either formation of a mirror pair must fail entirely, so one-way or no connections form - or the exchange of synaptic flux must flip-flop between exchanges predominantly in one direction

and then the other. An unstable fixed point of equilibrium will exist, and equation (10) becomes

$$\Delta\Phi^{+}(t) - \Delta\Phi^{-}(t) \to 0\,, \frac{dF}{dt} \to 0, and\ \frac{d^2F}{dt^2} \to +ve \qquad 11$$

Two consequences are:

(a) The asymmetry introduces a capacity for organization of chains of sequential activation, underlying the suggested operation of spinal segmental reflexes in Figure 1 and along the radial axes of development in the structural model.

(b) To the extent that the imperfectly matched areas achieve equilibrium of exchange, this must be at those temporal and spatial frequencies at which they are best matched.

3.2 Spatial frequency matching, and long and short ranges of axonal trees

Expanding (b) above a little more, maximization of zero-lag synchrony between mirror pairs requires matching at resonant temporal and spatial frequencies within each of the pair, so, during development, in the imperfect approach to mirror pairs between asymmetric cortical areas, spatial correlations of connections within each of the two areas must be approximated as closely as possible. This will then determine the patterns of interaction between areas at maturity.

A full treatment of spatiotemporal matching would need to consider shapes, orientation and relative size of the areas being matched, as well as the ranges of axonal connection and conduction rates. These difficulties can reduced to consideration of spatial frequency

matching in each of a mirror pair based solely on the axonal ranges of axons, from which special case the general case could be adduced.

The mirror pairs considered will be minimal model pairs of cortical areas, the axonal connections those in layer 2,3, and these further simplified into two cell populations – one with short axons representing local excitatory cells (similar in range to their local inhibitory cell partners) and one with longer axons, approximating superficial patch connections. The distribution of axon branches as a function of distances from cell bodies can be given as

$$\rho_\alpha = N_\alpha \lambda_\alpha \exp\left[-\lambda_\alpha x\right] \qquad 12$$

And

$$\rho_\beta = N_\beta \lambda_\beta \exp\left[-\lambda_\beta x\right] \qquad 13$$

where $\rho_\alpha(x), \rho_\beta(x)$ are the axonal tree densities of longer axon (alpha) cells, and shorter axon (beta) cells as a function of distance x from cell bodies. N_α, N_β are the fraction of cells in each population, and $\lambda_\alpha, \lambda_\beta$ are inverse length constants.

The distribution of spatial power within the cortical area will then be

$$P(k) = \left[\frac{N_\alpha \lambda_\alpha}{\pi(k + \lambda_\alpha^2)}\right]^2 + \left[\frac{N_\beta \lambda_\beta}{\pi\left(k + \lambda_\beta^2\right)}\right]^2 \qquad 14$$

where k is spatial frequency. From the spatial frequency spectrum the spatial auto and cross-correlation of the pattern of connections in a pair of cortical areas can be obtained via the Wiener-Khinchin theorem.

4. Simulating cortical growth within, and between, areas

Principles we have earlier used to simulate growth within a cortical area at mesoscale (Wright and Bourke 2016) can be applied to interareal development, to show how areas can become functionally merged, or kept functionally segregated.

4.1 Simulations of neocortical development at mesoscale in layers 2,3

Our simulations used axonal density as a function of range in the two axonal length populations in layer 2,3, as a measure of the synaptic flow neurones generate as a function of distance from the cell body. We exploited the dimensional analogy of synaptic flux to electric current or mechanical force to use a force minimization algorithm, establishing the positions at which all cell bodies in the simulated field would eventually be situated when, under the influence of Hebbian synaptic adjustments and apoptosis, they had reached equal and opposite exchanges of synaptic flux, and thus maximum synchrony.

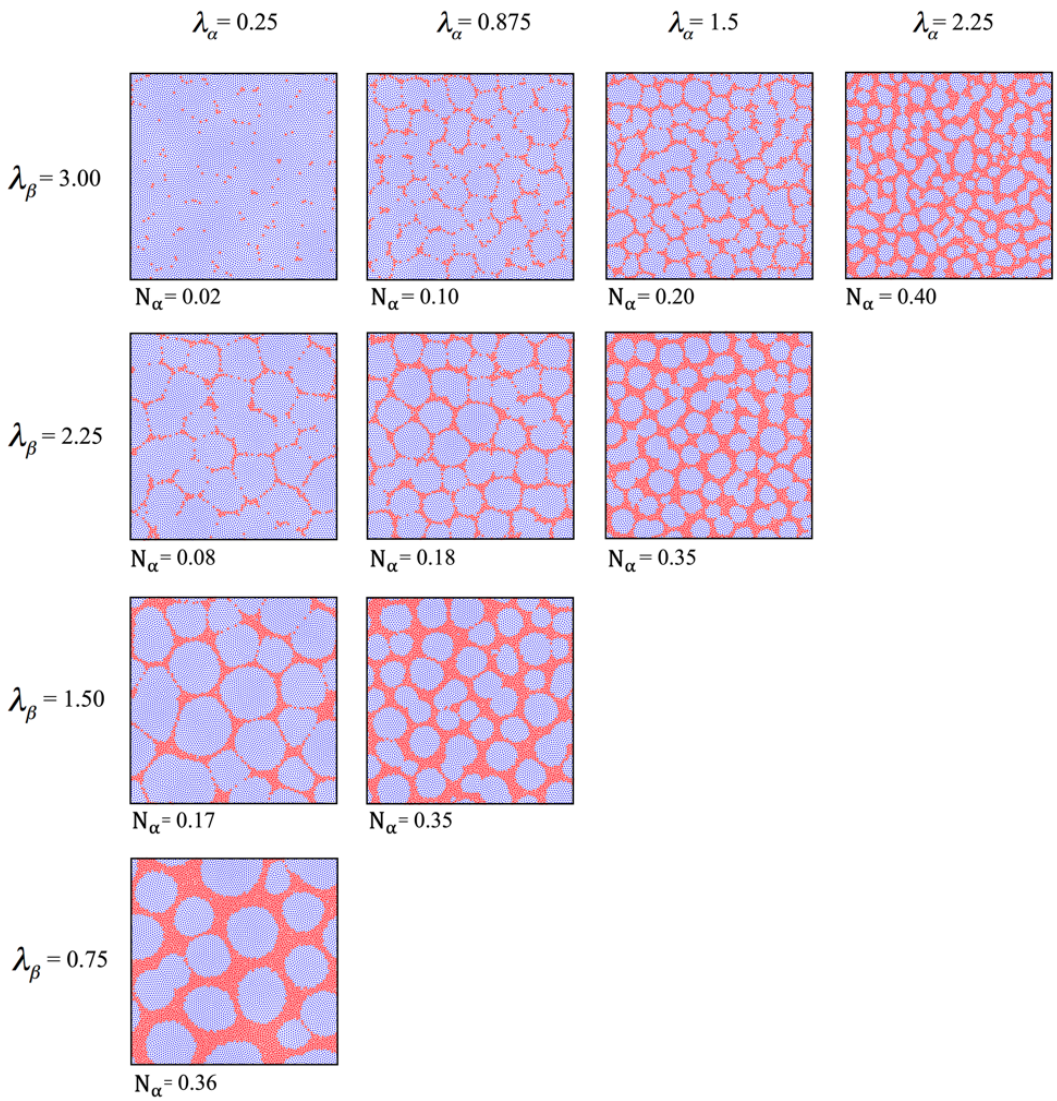

Figure 3.

Outcomes of growth simulations in a small cortical area as functions of axonal lengths, $\lambda_{\alpha,\beta}$. Red pixels – cell bodies of long axon cells. Blue pixels – cell bodies of short axon cells. Fraction of cells with long axons (N_α) are given for small world optimization with given axonal lengths .(From Wright and Bourke 2016)

Eight thousand points were distributed randomly in a 2 dimensional field, and a fraction, N_α, designated long axon alpha cells, coloured red, and a fraction, N_β, designated short axon

beta cells, coloured blue. The proportions of cells of each type were those best suited to assembly of a small world network, given specific ranges of long and short axons.

The polysynaptic synaptic fluxes passing between populations of cells of the same or different types can be expressed as aggregate forces, $S_{\alpha\alpha}, S_{\alpha\beta}, S_{\beta\alpha}, S_{\beta\beta}$. Because beta cells are more populous and have denser axonal trees at short range, in contrast to alpha cells at longer range, then aggregate effects sum to

$$S_{\beta\beta}(x) = \rho_\beta - \rho_\alpha = N_\beta \lambda_\beta e^{-\lambda_\beta x} - N_\alpha \lambda_\alpha e^{-\lambda_\alpha x} \quad 15$$

and

$$S_{\alpha\alpha}(x) = \rho_\alpha - \rho_\beta = N_\alpha \lambda_\alpha e^{-\lambda_\alpha x} - N_\beta \lambda_\beta e^{-\lambda_\beta x} \quad 16$$

and as synaptic weights become adjusted to maintain bidirectional equality of synaptic flux, $S_{\alpha\beta}(x) \to S_{\beta\alpha}(x) \to S_{\alpha\alpha}(x)$.

In the later stages of each simulation an expansive force, $G(x)$, was introduced to mimic the effects of cell divisions during growth with apoptosis, using the convenient arbitrary function

$$G(x) = \frac{1}{2}(1 - \sin\left(\frac{\pi}{2w}(x - w)\right) \quad 17$$

where w is range of growth or expansive force.

Outcomes of these simulations are reproduced in Figure 3. It can be seen that in all cases a columnar organization of beta cells has emerged, surrounded by alpha cells In a meshwork. The simulation method underestimates short-range connectivity among alpha cells, but with appropriate correction, approaches the pattern of superficial patch connections. (In the examples shown factors optimizing small world order were not applied, so that the columnar order is apparent in all cases. Although this ordering is always present it would be disguised by overlapping in some cases, creating the appearance of non-columnar cortex.)

4.2 Application of a similar method to ongoing development between cortical areas

As cortical areas are developing, cortico-cortical fibres bring them into mutual interaction. By the additive and dissipative wave effects described in section 2.5, each will impose upon the other signals with spectral characteristics determined by their axonal lengths (equations (12,13,14). By doing so they will modulate the growth effects within each other. One area may dominate over the other to a degree, k, where k ranges from 1-0. Labelling the two cortical areas A and B, and the local forces organizing each area $S(A,B)$

$$S(A,B) = S_{\alpha\alpha} + S_{\alpha\beta} + S_{\beta\alpha} + S_{\beta\beta} \qquad 18$$

the aggregate organizing forces operating on areas A and B including the imposed organization resulting from their relative cross-coupling, k, are

$$S_k(A) = kS(A) + (1-k)S(B) \qquad 19$$

on area A, and on area B

$$S_k(B) = (1-k)S(A) + kS(B) \qquad 20$$

With this modification, simulations of growth in coupled areas can then use the same method as for single areas.

5. The emergence of interareal cross-connections

5.1 Initial conditions and auto and cross-correlations in some specific comparisons

In Figure 4 simulation outcomes for two simulated cortical areas, A and B, show the effects of cross-linkage or its absence, and the effects of same or different initial connections. A and B have parameters drawn from two cases among those shown in Figure 3. These two instances differ in the range parameters of the axonal trees (λ_α and λ_β) but have the same proportions of long and short axon neurons – ie, N_α, N_β are identical in A and B. Differences in the effects of same or differing external inputs were emulated by using the same or different initial seed values for the randomised placements of cells prior to the initiation of force equilibration in the simulations.

In the first row of Figure 4 it can be seen that although no cross-coupling has been applied between A and B, the similar input/initial condition results in similar spatial autocorrelations, and partial cross correlation, of A and B.

In the second row the same input/initial condition applies, but equations (18-20) have been brought into operation with k = 0.5. That is, A and B interact equally and strongly during "neurogenesis". Despite differences in the axonal lengths in A and B, the outcome is their complete spatial correspondence and maximal mutual information.

The third and fourth rows show that when inputs/initial conditions differ, whether cross-coupled or uncoupled, no spatial correspondences or mutual information arise between A and B.

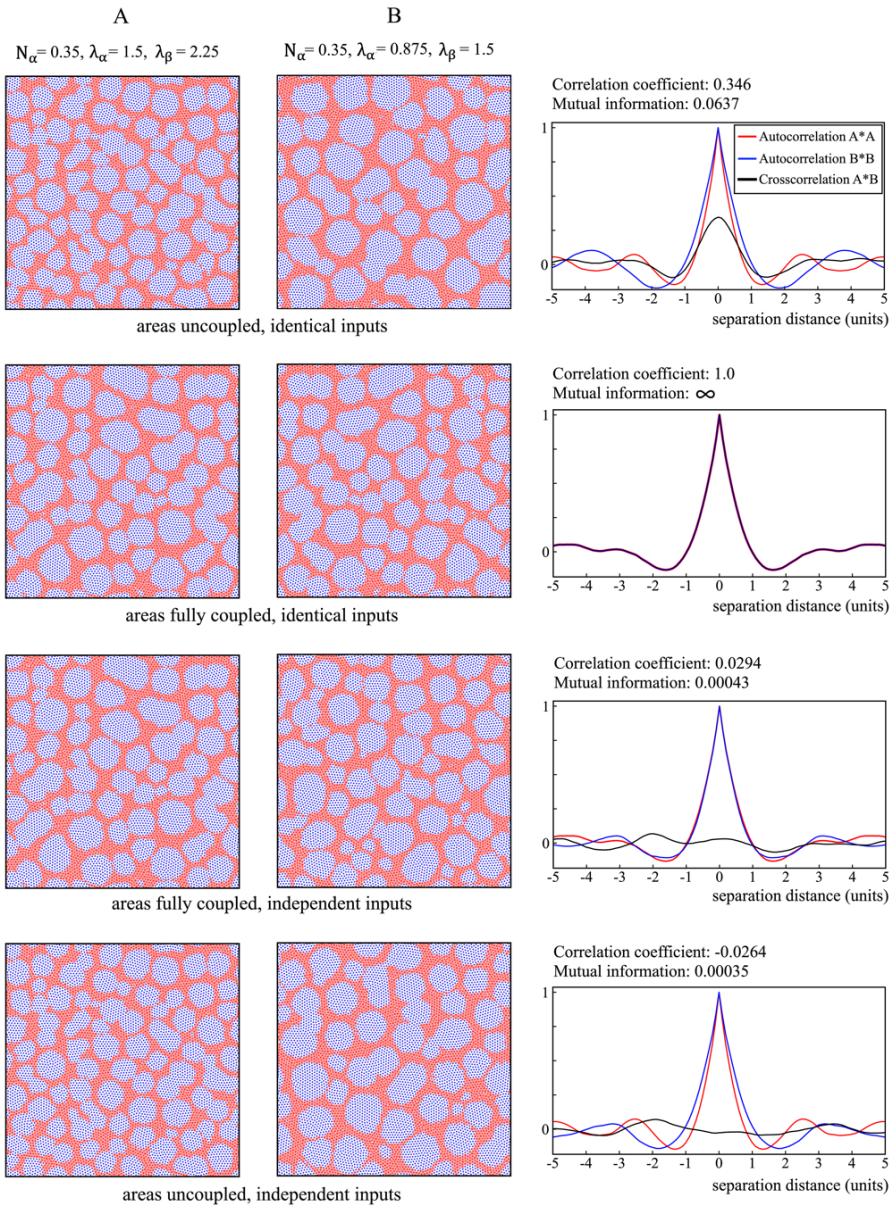

Figure 4.

Simulations of two cortical areas, A and B, with differing axonal lengths but the same fractions of long versus short axon cells. Effects of differing versus identical inputs, and of full coupling versus absence of coupling, upon spatial auto- and cross-correlations

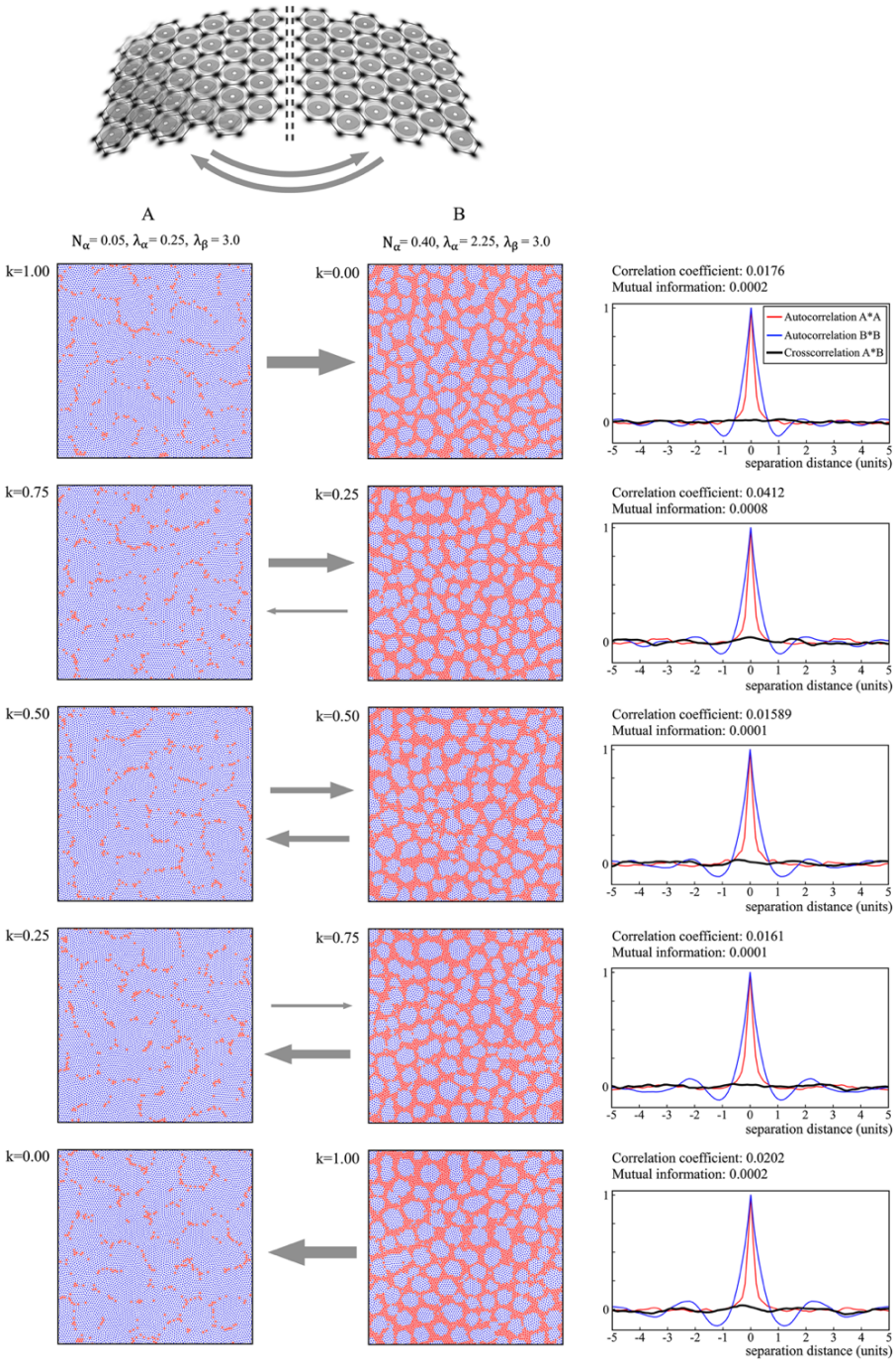

Figure 5.

Simulation outcomes with identical inputs where the fractions of long versus short axon cell, N_α, as well as the axonal lengths, $\lambda_{\alpha,\beta}$, are highly disparate between A and B. Dark grey arrows between simulation pairs indicate the relative strengths of coupling of cortico-cortical connections in each direction of synaptic flow. Cross-correlations are effectively zero in all coupling conditions.

Figure 5, and Figure 6, extends the comparison to further paired examples drawn from Figure 3, to highlight differences in outcome related to the strength and direction of cross coupling between A and B (parameter k) and also to differences in the ratios of long and short axon cells (N_α, N_β). In all comparisons input/initial cell positions were identical in A and B.

In Figure 5, where disparity in parameters N_α, N_β are large, it can be seen that while spatial autocorrelations remain similar, cross-correlations, and mutual information remain effectively zero for all values of k, including $k = 0.5$.

In Figure 6, as in Figure 4, A and B share the same values of N_α, N_β, but again with disparate $\lambda_\alpha, \lambda_\beta$. It can be seen that spatial cross-correlation and mutual information reaches the limit for the case that $k = 0.5$, when cross-linkage is opposite and equal, but some cross-correlation is apparent wherever some degree of bilateral, but asymmetric, cross-coupling is present.

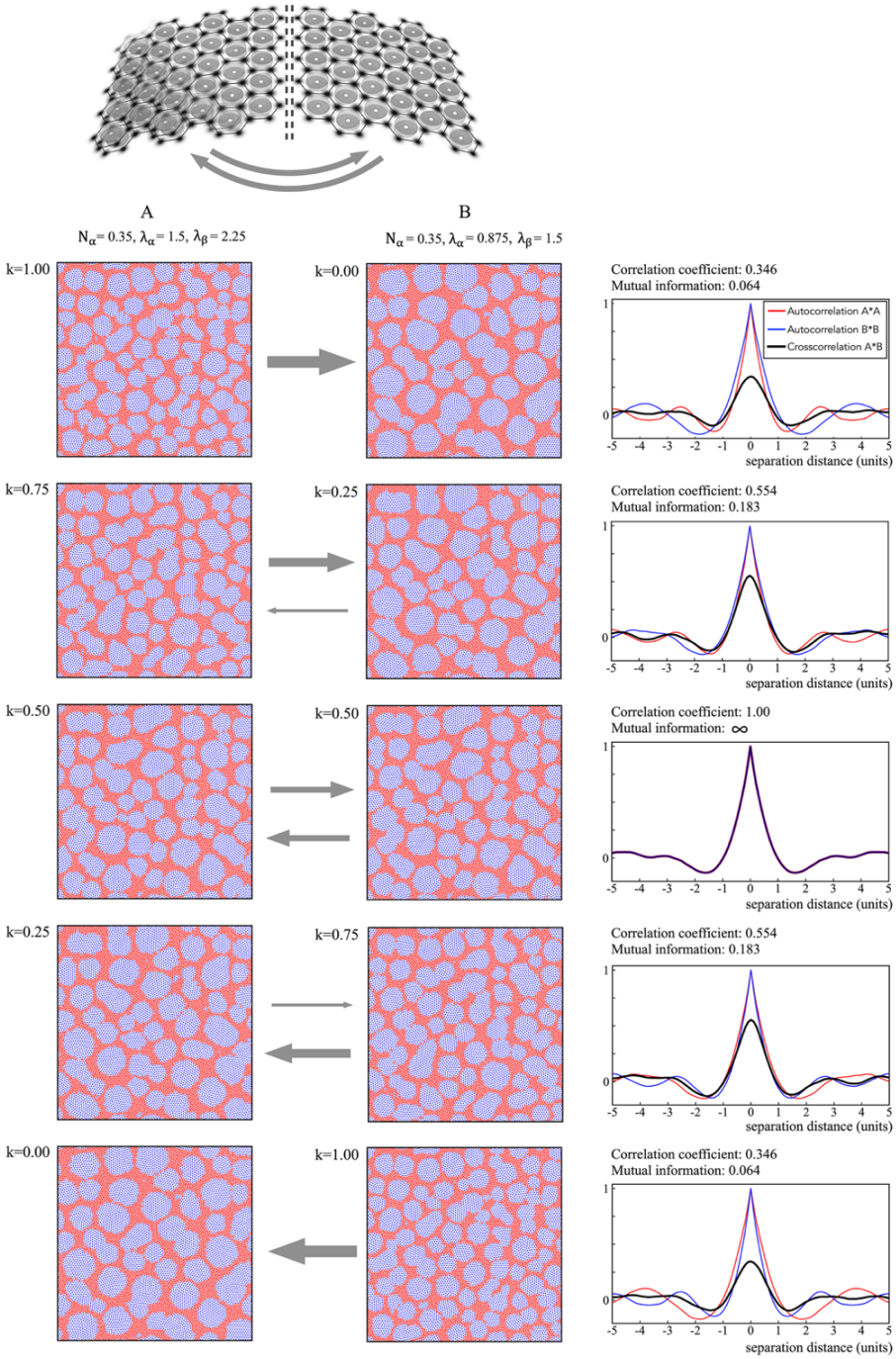

Figure 6.

Simulation outcomes in the same format as Figure 5. In this case, although the axonal lengths, $\lambda_{\alpha,\beta}$, are disparate, the fractions of long versus short axon cells, N_α, are identical. Cross correlations are now higher in all conditions of cross-coupling, and with bidirectional equal cross-coupling, outcomes in A and B are identical.

5.2 Systematic analyses in representative examples

To permit convenient comparisons of degree of match or mismatch of asymmetric cortical areas, we took advantage of a property of the spatial power spectrum; equation (14). Since $N_\alpha = 1 - N_\beta$, then if $\lambda_\alpha, \lambda_\beta$ are given for two cortical areas, adjustment of their values of N_α will permit their cross-correlation to be adjusted into closer or lesser approximation. The disparity between actual values of N_α applying in A and B, and the optimum value to match the power spectra of A and B is thus a measure of match or mismatch of initial conditions, and will exert effects comparable to superadded noise, from whatever source – a comparison confirmed using actual overlaid noise in other simulations (not reported). We use the term "Long Axon Fraction (LAF)" to represent the adjusted values of N_α, to distinguish the adjusted fraction from the small-world optimum N_α of each simulation. Figure 7 uses this measure, and variation of the cross-coupling parameter, k, in a set of paired A and B comparisons. Initial conditions set by randomization were identical left and right, to model comparability of external (thalamic) inputs in development.

In 7 (a) cases A and B have identical values of $N_\alpha, N_\beta, \lambda_\alpha, \lambda_\beta$. Outcomes are identical in A and B. Their spatial cross-correlation is exact, r=1, for all values of cross-coupling, and there is no LAF disparity between the values of N_α in A and B. They have maximum mutual information in all conditions.

In 7 (b) cases A and B remain matched for the value of N_α, N_β, but differ in the values of fibre ranges, $\lambda_\alpha, \lambda_\beta$. Now the maximum $r = 1$ is reached only when $k = 0.5$, when A and B exert equal and opposite effects of A upon B and vice-versa. Again, there are no LAF

disparities. However, approach to high mutual information would depend upon close balance of signal exchanges brought about by external controls.

In 7 (c) there is some mismatch of N_α, N_β in A and B, and the peak $r = 1$ at $k = 0.5$ is disparate in LAF from the correct matching values of N_α. There remains a zone of cross-correlation, maximal at $k = 0.5$, but $r \neq 1$. Matching of mutual information between areas is restricted, compared to (a) and (b).

In 7 (d) the LAF disparity in A and B is now extreme, and under no combinations of cross-couplings are there discernible spatial cross-correlations. Mutual information of A and B is effectively zero.

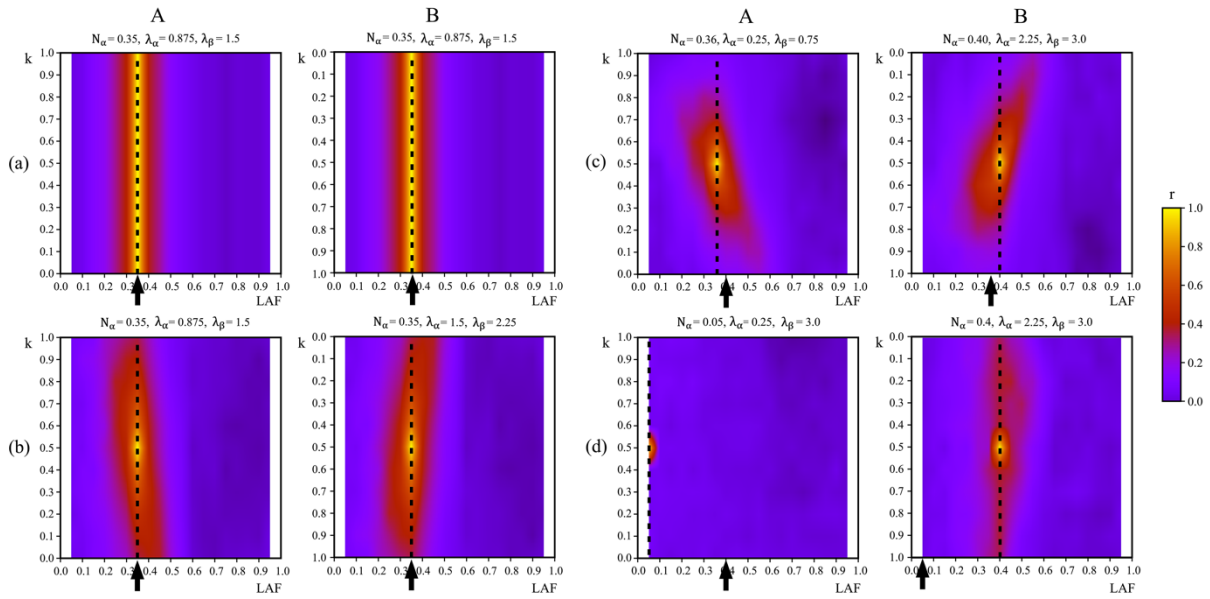

Figure 7.

Plots of cross-correlation, r, versus cross-coupling, k, for selected A and B pairs with graded disparities in N_α, and in $\lambda_{\alpha,\beta}$. Spatial frequencies in A and B have been varied by adjustment of N_α away from the correct value for the given parameters of the simulation, shown as

position on LAF axes. The vertical dashed lines mark the correct value of N_α for A or for B, and the black arrows mark the correct value for the opposite member of the A and B pair – measuring disparity of their matching.

6. Conclusion

These results extend prior concepts of radial and meso-scale self-organization in neocortex to include circumferential cortico-cortical connectivity. Built upon a primarily radial and hierarchical order of the structural model, a preliminary explanation for the complexities of the Brodmann areas, and Yeo areas can be sketched out. Arising developmentally, there is a continuum of possible relationships between cortical areas. At one extreme are those areas closely approaching mirror symmetry and interacting strongly at all levels of cortical activation. Intermediate cases are those that can be brought into functional interaction by adjustments of their excitation toward equality ($k = 0.5$). At the other extreme, are those with limited or absent symmetry and/or low levels of information exchange, that are able to operate effectively independently.

6.1 Overall cortical development

As cortico-cortical connections form according to the distance rule of separation, those areas that receive shared information from external sources, and have intracortical axonal fibre ranges sufficiently similar in both areas to match spatial frequencies each with the other, will begin to interact, increasing the level of their coupling, maximizing their mutual information, and accounting for the features listed by Goldman-Rakic cited in the Introduction. This applies, to greater or lesser degree to all cortical areas in which mirror symmetries are apparent, as is seen for example in the sequence of visual areas, and

between left and right visual cortex. Conversely, cortical areas that do not share common inputs, and/or have differing spatial and temporal patterns of activity will not form cross-connections. This will enable separated cortical areas to serve specialised functions within the global order of neocortical operations.

The segregation of cortical areas will therefore be, to some degree, a separation of areas with low temporal and spatial frequencies versus high frequencies, and this implies two further properties: (a) the specialization of high frequency areas on local and rapid sequences of information processing, and specialization of low frequency areas on slower, more extensive processing; favouring (b) supervisory coordination of high frequency areas by low frequency areas. This kind of supervision would pertain, broadly, to left versus right hemispheres, and to the predominance in dorsal neocortex, with distributed coordination of neurones selective for shape perception and movement control, over the finer definition of stimulus/perceptual objects in ventral cortex. Co-ordination of high frequency systems by lower frequency systems would apply similarly at meso-scale, where “like to like” superficial patch system connections co-ordinate interactions among stimulus-tuned neurons.

Networks operating in parallel and in different sequences would overcome the information processing limitations of predictive error minimization in hierarchical radial sequences alone, and permit chained cognitive sequences of indefinite time duration.

6.2 Sequences of cortical activity and their control

As development proceeds to a mature stage, control of Interareal flows from subcortical sources would regulate the flip-flopping of synaptic flux over unstable fixed points of

intervening Markov blankets by two mechanisms. Firstly, the mean level of activation in any two areas, would regulate parameter k – ie: the strength and directionality of signal flow between areas, and by tuning to $k = 0.5$, would optimize interaction. Secondly, the rules of synchrony generation and wave interactions described in section 2.5, allow for modulation cortical activity at the rhythms at the theta, alpha, and beta frequencies. This accords with a recent theoretical analysis (Tucker and Luu 2026) arguing that excitatory tone from hypothalamic/hippocampal sources, modulated at theta frequency, and from thalamic and basal ganglia circuits at beta frequency, is delivered in limbifugal flows along cortical layers 5/6, interacting with gamma activity in an oppositely directed limbipetal flow. Lower level generation of oscillating signals at these lower frequencies would arise in the same way as at the gamma frequency, but with longer delays in the excitatory/inhibitory to-and-fro exchanges. A major inference drawn by Tucker and Luu is that internal modulation of the counterflows would result in transient but widespread synchronous fields, with a duration enabling NMDA-mediated strengthening of synaptic connections so as to establish a memory trace.

6.3 Summing up

A consistent multilevel account of prediction error and active inference, under active affordance can be advanced, in which synchronous oscillation is the universal attractor. Cell organizations trend to mirror pair symmetries, but broken symmetries allow sequences of area-specialised spatiotemporal sequences within the total flow. This account is applicable within current accounts of the overall structure of the brain. Biologically, the selection among developing neurons of ensembles that fire in zero-lag synchrony drives the process of self-organization.

This model is included within the wider context of self-organizing non-equilibrium physical systems, and the linkage of all such systems to active inference and the free energy principle can again be emphasised.

Acknowledgements

This work arose from long-term support including that of the Frank Hixon Fund of the California Institute of Technology, the Mental Health Research Fund, and Wellcome Trust in the UK, the United Kingdom, New Zealand, and Australian Medical Research Councils, and the Oakley, and Pratt, Foundations of Australasia.

Appendix. *Mirror systems at mesoscale.*

Figure A shows the geometrical forms within neocortex that can be accounted for as mirror symmetries.

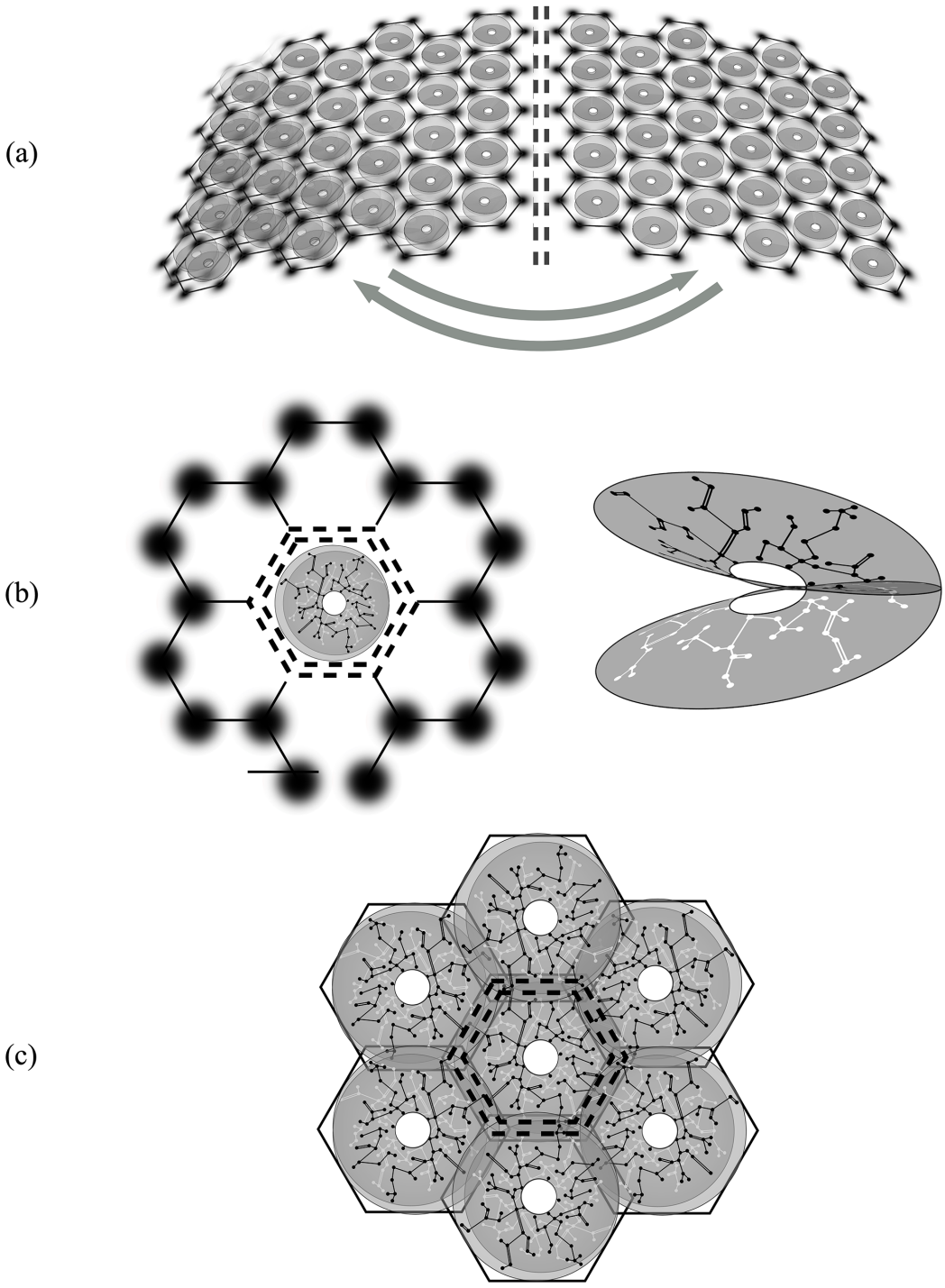

Figure A.

(a) Within cortical areas columns arise at mesoscale, with mirror symmetry. In the small area bottom left of the cortical areas, the columns are shown blurred into each other, as a reminder that column formation need not be anatomically distinct.

(b) *left. Superficial patch connections surround and interconnect columnar zones in layers 2,3, as seen in cortical surface view, producing between-scale mirroring.*

(b) *right. Cells of the columnar zone in cortical depth. Maximization of synchrony in interpenetrating sparsely coupled networks leads to multiple closed loop systems akin to Mobius strips.*

(c) *Adjacent columns become arranged in approximate mirror symmetry, each with its neighbours.*

Applications of the theory of synchrony maximization and mirror formation (Wright and Bourke 2013, 2016, 2022, Wright et al 2014) explain the following experimental observations:

- Columnar versus noncolumnar variation (Horton and Adams 2005, Muir et al. 2011, Muir and Douglas 2011, Molnar 2013).
- The antenatal development of retinotopic maps (Wiesel and Hubel 1974, and their postnatal loss with deprivation of visual experience (Blakemore and Van Sluyters 1974, Espinosa and Stryker 2012, Konkle 2021).
- Differential shape and movement sensitivities in dorsal versus ventral neocortex (Trevarthan 1868,Ungeleider and Mishkin 1982, Goodale and Milner 1992)
- Retinotopic response maps in cortical area V1 – Orientation Preference (OP) singularities, linear zones and saddle points (Bosking et al. 1997, Girman et al.1999, Levitt and Lund 2002, Obermayer and Blasdel 1993). Mobius-like internal configuration within a column accounts for the organization of OP from 0 – 180 degrees over the 360 degrees around an OP singularity. Linear zones and saddle points of OP are accounted for by mirror symmetric reversals with some broken symmetry at columnar boundaries.

- Ocular dominance (OD) columns in square array (Obermayer and Blasdel 1993).
- “Like to like” patch cell connections – ie: the preferential connections of patch cells to columnar cells with a common OP (Rockland and Lund 1983, Levitt and Lund 2002, Martin et al 2014, Chavane et al. 2022).
- The numerical relationship TFP = object velocity x SFP between preferred spatial frequency (SFP) and preferred temporal frequency (TFP) in individual cortical neurones (Baker 1990, Zhang et al. 2007, Issa et al. 2000, 2008).
- The differential distribution of SFP and TFP in relation to OP (Issa 2008).
- OP variation in response to moving line stimuli of given orientation, and varied speed, angle of attack, and length (Basole et al 2003) – an effect of intracortical contextual connections, in contrast to OP selection on the input pathway alone (Vidyasagar and Eysel 2015).
- Recordings made by vertical penetrations of somatosensory cortex showing that receptor fields for cells have continuities of the fields as the recording electrode is advanced, and sudden breaks and reversal of continuity – consistent with the organization of local cell connections in Mobius-like configuration spiralling within the cortical layers and the occurrence of mosaic connectivity in cortical columns (Miyashita 2025).

References

Adams RA, Shipp S, Friston K. Predictions not commands:active inference in the motor system. *Brain Struct. Funct.* 2013: 218: 611-643. doi.org 10.1007/s00429-012-0475-5

Amsterdam: Elsevier. 2020 doi:10.1016/B978-0-12-397267-5.00137-0

Aparicio-Rodriguez G, Garcia-Cabezas MA Comparison of the predictive power of two models of cortico-cortical connections in primates: the distance rule model and the structural model. *Cerebral Cortex* 2023:33: 8131-8149. doi:10.1093/cercor/bhad104

Baker CL. Spatial- and temporal-frequency selectivity as a basis for velocity preference in cat striate cortex neurons. *Vis. Neurosci*. 1990: 4 :101–113. doi: 10.1017/S0952523800002273

Barbas H, Garcia-Cabezas MA (2016) How the prefrontal executive got its stripes. *Curr. Opin. Neurobiol.* 2016: 40: 125-134. doi:10.1016/j.conb.2016.07.003

Barbas H, Garcia-Carbezas MA. Motor cortex layer 4 : less is more. *Trends Neurosci.* 2015: 38: 259-261. doi:10.1016/j.tins.2015.03.005

Barbas H, Rempel-Clower N. Cortical structure predicts the pattern of cortico-cortical connections. *Cerebral Cortex* 1997:7:635-646. doi: 10.1093/cercor/7.7.635

Barbas H. General cortical and special prefrontal connections: principles from structure to function. *Annual Rev Neuroscience* 2015: 38: 269-289. doi: 10.1146/annurev-neuro-071714-033936.

Barbas H. Pattern in the laminar origin of cortico-cortical connections *J Comp Neurol* 1986 :252:415-422. doi: 10.1002/cne.902520310

Basole A, White LE, Fitzpatrick D. Mapping of multiple features in the population response of visual cortex. *Nature* 2003: 423: 986–990. doi:1038/nature01721

Bassett DS, Bullmore, E. Small-world brain networks. *Neuroscientist* 2006:12:512-513. doi:10.1177/1073858406293182

Bastos AM, Lundkqvist M. Waite AS, Miller EK. Layer and rhythm specificity for predictive routing. *PNAS* 2020:117: 31459-31469. doi.org/10.1073/pnas.2014868117

Bastos AM, Usrey WM, Adams RA, Mangun GR, Fries P, Friston KF. Canonical microcircuits for predictive coding *Neuron* 2012: 76: 695-711. doi:10.1016/j.neuron.2012.10.038

Blakemore C, Van Sluyters RC. Reversal of the physiological effects of monocular deprivation in kittens: Further evidence for a sensitive period. *J. Physiol.* 1974: 237:195–216. doi: 10.1113/jphysiol.1974.sp010478

Bosking WH, Zhang Y, Schofield B, Fitzpatrick D. Orientation selectivity and the arrangement of horizontal connections in tree shrew striate cortex. *J Neurosci* 1997: 17: 2112-2127. doi:10.1523/JNEUROSCI.17-06-02112.1997

Brodmann K. Vergleichende Lokalisationslehre der Grosshirnrinde . Leipzig: Johann Ambrosius Barth. 1909

Breakspear M. Nonlinear phase desynchronization in human electroencephalographic data. Hum Brain Mapp 2002: 15, 175-198. doi: 10.1002/hbm.10011

Breakspear M. "Dynamic" connectivity in neural systems: theoretical and empirical considerations. Neuroinformatics 2004: 2, 205-226. doi: 10.1385/NI:2:2:205.

Breakspear M, Stam CJ. Dynamics of a neural system with a multiscale architecture. Philosophical transactions of the Royal Society of London. Series B, Biological sciences. 2005: 360, 1051-1074.doi: 10.1098/rstb.2005.1643

Buckley CL, Kim CS., McGregor S, Seth AK. The free energy principle for action and perception: a mathematical review. *J. Math. Psychol.* 2017: 81: 55–79. doi: 10.1016/j.jmp.2017.09.004

Butler AB. Evolution of the thalamus: a morphological and functional review. *Thalamus Relat Syst.* 2008: 4: 35-58. doi:10.1017/S1472928808000356

Chapman CL, Wright JJ, Bourke PD. Spatial eigenmodes and synchronous oscillation: coincidence detection in simulated cerebral cortex. *J. Math. Biol.* 2002: 45: 57-78. doi:10.1007/s002850200141

Chavane F, Perrinet LU, Rankin J. Revisiting horizontal connectivity rules in V1. *Brain Struct Funct* 2022: 227: 1279-1295. doi:10.1007/s00429-022-02455-4

Cisek P. Evolution of behavioural control from chordates to primates. Phil. Trans R. Soc. B.2022: 377: 20200522. doi.org/10.1098/rstb.2020.0522

Conant RC, Ashby WR. Every Good Regulator of a system must be a model of that system. *Int. J. Systems Sci.* 1970 :1: 89-97. doi:10.1080/00207727008920220

Downes JH, Hammond MW, Xydas D, Spencer MC, Becerra VM, Warwick K, Whalley BJ, Natsuto SJ. Emergence of a small-world functional network in cultured neurons. *PLoS Comput. Biol.* 2012: 8:e1002522. doi: 10.1371/journal.pcbi.1002522

Espinosa JS, Stryker MP. Development and plasticity of the primary visual cortex. *Neuron* 2012: 75: 230–249. doi: 10.1016/j.neuron.2012.06.009

Formisano E, Kim D-S, Di Salle F, van de Moortele P-F, Ugurbil K, Goebel R. Mirror-symmetric tonotopic maps in human primary auditory cortex. *Neuron* 2003 40: 859-869 doi.org/10.1016/S0869-6273(03)00669-X

Friston K, Ao P. Free energy, value, and attractors. *Comput. Math. Methods Med*. 2012: 937860. doi: 10.1155/2012/937860

Friston K, Buzsaki G. The Functional Anatomy of Time: What and When in the Brain. *Trends Cogn Sci* 2016 : 20 : 500-511. doi:10.1016/j.tics.2016.05.001

Friston K, Parr T, Yufik Y, Sajid N, Price CJ., Holmes E. Generative models, linguistic communication and active inference. *Neurosci. Biobehav. Rev.* 2020: 118: 42–64. doi: 10.1016/j.neubiorev.2020.07.005

Friston K, Da Costa L, Sakthivadivel DAR, Heins C, Pavliotis GA, Ramstead M, Parr T. Path integrals, particular kinds, and strange things. Physics of Life Reviews 2023: 47, 35-62. doi.org/10.1016/j.plrev.2023.08.016

Friston K. A theory of cortical responses. *Philos. Trans. R Soc. B Biol. Sci.* 2005: 360: 815–836. doi: 10.1098/rstb.2005.1622

Friston K. Functional integration and inference in the brain. *Prog. Neurobiol.* 2002: 68: 113–143. doi: 10.1016/S0301-0082(02)00076-X

Friston K. Hierarchical models in the brain. *PLoS Comput Biol* 2008:4: e1000211.

Friston K. Maps and territories, smoke and mirrors. *Behav. Brain Sci*. 2022: 45: e195. doi: 10.1017/S0140525X22000073

Friston K. The free energy principle: a unified brain theory? *Nat. Rev. Neurosci*. 2010 : 11 : 127–138. doi: 10.1038/nrn2787

Friston KJ, Fagerholm ED, Zarghami TS, Parr T, Hipolito I, Magrou L, Razo A. Parcels and particles: Markov blankets in the brain. *Network Neuroscience.* 2021: 5: 211-251. doi.org/10.1162/netn_a_00175

Friston K, Frith C. A Duet for one. Conscious Cogn 2015: 36, 390-405. doi:10.1016/j.concog.2014.12.003

Friston KJ, Parr T, de Vries B., 2017. The graphical brain: Belief propagation and active inference. *Network Neuroscience (Cambridge, Mass.)* 2017: 1: 381-414. doi:10.1162/NETN_a_00018

Friston KJ, Shiner T, FitzGerald T, Galea JM, Adams R, Brown H, Dolan RJ, Moran R, Stephan KE, Bestmann S. Dopamine, affordance and active inference. *PLOS Computational Biology* 2012: 8: e1002327 doi.org/10.1371/journal.pcbi.1002327

Froudist-Walsh S, Xu T, Niu M, Rapan L, Zhao L, Margulies DS, Zilles K, Wang X-J, Palomero-Gallagher N. Gradients of neurotransmitter receptor expression in the macaque cortex. *Nature Neuroscience* 2023: 26: 1281-1294. doi.org/10.1038/s41593-023-01351-2

Garcia-Cabezas MÁ, Hacker JL, Zikopoulos B. A protocol for cortical type analysis of the human neocortex applied on histological samples, the Atlas of Von Economo and Koskinas, and magnetic resonance imaging. *Front Neuroanat* 2020: 14: 576015. doi:10.3389/fnana.2020.576015

Garcia-Cabezas MA, Joyce MKP, John YJ, Zikopoulos B, Barbas H. Mirror trends of plasticity and stability indicators in primate prefrontal cortex. *Eur J Neurosci* 2017: 46: 2392-2405. doi:10.1111/ejn.13706

Garcia-Cabezas MA, Zikopoulos B, Barbas H. The structural model : a theory linking connections, plasticity, pathology, development and evolution of the cerebral cortex. *Brain Struct. Function* 2019: 224: 985-1008. doi: 10.1007/s00429-019-01841-9.

Garcia-Carbezas MA, Barbas H. Area 4 has layer IV in adult primates. *Eur J Neuroscience* 2014: 39: 1824-1834. doi:10.1111/ejn.12585

Girman SV, Sauve Y, Lund RD. Receptive field properties of single neurons in rat primary visual cortex *J Neurophysiol.* 1999: 82: 301-311. doi:10.1152/jn.1999.82.1.301

Goldman-Rakic PS. Topography of cognition: parallel distributed networks in primate association cortex. Annu Rev Neurosci. !988 11: 137–156 doi:10.1146/annurev.ne.11.030188.001033

Goodale MA, Milner AD. Separate visual pathways for perception and action. *Trends in Neurosciences* 1992: 15: 20-25 doi.org/10.1016/0166-2236(92)90344-8

Hansen JY, Shafiei G, Markello RD, Smart K, Cox SML, Norgaard M, Beliveau V, Wu Y, Gallezot J-D, Aumont E, Servaes S, Scala SG, DuBois JM, Wainstein G, Bezgin G, Funck T, Schmitz TW, Spreng RN, Galovic M, Koepp MJ, Duncan JS, Coles JP, Fryer TD, Aigbirhio FI,

MacGinnity CJ, Hammers A, Soucy J-P, Baillet S, Guimond S, Hietala J, Bedard M-A, Leyton M, Kobayashi E, Rosa-Net P, Ganz M, Knudsen GM, Palomera-Gallaher N, Shine JM, Carson RE, Tuominen L, Dagher A, Misic B. . Mapping neurotransmitter systems to the structural and functional organization of the human neocortex. *Nature Neuroscience* 2022: 25: 1569-1581. doi.org/10.1038/s41593-022-01186-3

Heck N, Golbs A, Riedemann T, Sun J-J, Lessman V, Luhmann HJ. Activity dependent regulation of neuronal apoptosis in neonatal mouse cerebral cortex. *Cerebral Cortex* 2008: 18: 1335–1349. doi:10.1093/cercor/bhm165

Hohwy J. The Self-Evidencing Brain. *Nous* 2016: 50: 259-285. doi.org/10.1111/nous.12062

Hollville E, Romero SE, Deshmukh M. Apoptotic cell death regulation in neurons. *FEBS J*. 2019: 286: 3276-3298. doi:10.1111/febs.14970

Horton JC, Adams DL The cortical column: a structure without a function. *Philosophical Trans Royal Soc.* 2005: 360: 837-862. doi:10.1098/rstb.2005.16232013

Issa NP, Rosenberg A, Hussson TR. Models and measurements of functional maps in V1. J. Neurophysiol. 2008: 99 :2754–2754. doi:10.1152/jn.90211.2008

Issa NP, Trepel C, Stryker MP. (2000). Spatial frequency maps in cat visual cortex. *J. Neurosci*. 2000 : 20 : 8504–8514. doi:10.1523/JNEUROSCI.20-22-08504.2000

Ito J., Kaneko K. Self-organized hierarchical structure in a plastic network of chaotic units. Neural Networks 2000: 13, 275-281. doi.org/10.1016/S0893-6080(99)00107-0

Jafri HH, Singh RK, Ramaswamy R. Generalized synchrony of coupled stochastic processes with multiplicative noise. Phys Rev E 2016: 94, 052216.doi: 10.1103/PhysRevE.94.052216

Jarzynski C. Nonequilibrium equality for free energy differences. Physical Review Letters 1997: 78, 2690-2693. doi.org/10.1103/PhysRevLett.78.2690

Jiang D-Q, Qian M, Qian M-P. (2004). Mathematical theory of nonequilibrium steady-states. Springer. ISBN 3540409572,97835440409571

Izhikevich EM, Desai NS. Relating STDP to BCM. *Neural. Comput.* 2003 : 15 : 1511–1523. doi: 10.1162/089976603321891783

Keck T, Toyoizumi T, Chen L, Doiron B, Feldman DE, Fox K, Gerstner W, Haydon PG, Hubener M, Lee H-K, Lisman JE, Rose T, Sengpiel F, Stellwagen D, Stryker MP. Integrating Hebbian and homeostatic plasticity: the current state of the field and future research directions. *Philosoph. Trans. Royal Society B.* 2017: 327: 1715. doi:10.1098/rstb.2016.0158

Kirchhoff M, Parr T, Palacious E, Friston K, Kiverstein J. The Markov blankets of life: autonomy, active inference and the free energy principle. *Journal of the Royal Society Interface* 2018 doi:10.1098/rsif.2017.0792

Konkle T. Emergent organization of multiple visuotopic maps without a feature hierarchy. *bioRxiv* 2021 doi:10.1101/2021.01.05.425426

Kwisthout J, van Rooij I. Computation resource demands of a predictive Bayesian brain. *Computational Brain and Behaviour.* 2020 3: 174-188.

Springer.com/article/10.1007/s42113-019-00032-3

Kwon C, Ao P. Nonequilibrium steady state of a stochastic system driven by a nonlinear drift force. Physical Review E. 2011: 84, 061106. doi.org/10.1103/PhysRevE.84.061106

Levitt JB, Lund JS. Intrinsic connections in mammalian cerebral cortex. In: *Cortical Areas (2002) CRC Press* eBook ISBN 9780429219108

Loonen AJM, Ivanova SA. Circuits regulating pleasure and happiness. The evolution of the amygdala-hippocampal-habenular connectivity in vertebrates. *Front. Neurosci.* 2016: 10: 539 doi:10.3389/fnins.2016.00539

Lungarella M, Sporns O. 2006. Mapping information flow in sensorimotor networks. PLoS Comput Biol 2006: 2, e144. doi.org/10.1371/journal.pcbi.0020144

Luu P, Tucker DM, Friston K. From active affordance to active inference: vertical integration of cognition in the cerebral cortex through dual subcortical control systems. *Cerebral Cortex* 2024: 34: bhad458. doi:10.1093/cercor/bhad458

Luu P, Tucker D, Friston K. The organizational basis of active affordance: evidence from structural and prosomeric models of the neuraxis. *Cerebral Cortex* 2026 (in review)

Markov NT, Misery P, Falchier A, Lamy C, Vezoli J, Quilodran R, Gariel MA, Giroud P, Ercsey-Ravasz M, Pilaz LJ, Huissoud C, Barone P, Dehay C, Toroczkai Z, Van Essen DC, Kennedy H, Knoblaunch K. Weight consistency specifies regularities of macaque cortical networks. *Cerebral Cortex* 2011: 21: 1254-1272. doi: 10.1093/cercor/bhq201

Martin KAC, Roth S, Rusch ES. Superficial layer pyramidal cells communicate heterogeneously between multiple functional domains of cat primary visual cortex *Nature Communication* 2014: 55252. doi:10.1038/ncommns6252

Miller KD. Synaptic economics: competition and cooperation in synaptic plasticity. *Neuron* 1996: 17: 371-374 doi:10.1016/S0896-6273(00)80169-5

Molnar Z. Cortical columns. In: Rubenstein JLR. and Rakic P. (ed.) Comprehensive Developmental Neuroscience: Neural Circuit Development and Function in the Brain. 2013 :vol 3, pp. 109-129 doi: 10.1016/B978-0-12-397267-5.00137-0

Muir DR, Da Costa NMA, Girardin CC, Naaman S, Omer DB, Ruesch E, Grinvald A, Douglas RJ. Embedding of cortical representations by the superficial patch system. *Cerebral Cortex* 2011: 21: 2244-2260. doi:10.1093/cercor/bhq290

Muir DR, Douglas RJ. From neural arbours to daisies. *Cerebral Cortex* 2011: 21: 1118-1133 doi:10.1093/cercor/bhq184

Miyashita T. Complicated architecture of cortical microcircuit: a comprehensive review. *Anatomical Science International* 2025: doi.org/10.1007/s12565-025-00877-8

Namikawa J. Chaotic itinerancy and power-law residence time distribution in stochastic dynamical systems. Physical review E. 2005: 72, 026204. doi.org/10.1103/PhysRevE.72.026204

Nara S. Can potentially useful dynamics to solve complex problems emerge from constrained chaos and/or chaotic itinerancy? Chaos 2003: 13, 1110-1121. doi.org/10.1063/1.1604251

Nicolis G, Prigogine I. (1977). Self-organization in nonequilibrium systems : from dissipative structures to order through fluctuations. Wiley, New York. doi.org/10.1002/bbpc.197800155

Nieuwenhuys R. The structural, functional, and molecular organization of the brainstem. *Frontiers in neuroanatomy* 2011 5:33. doi.org/10.3389/fnana.2011.00033

Obermayer K, Blasdel GG. Geometry of orientation and ocular dominance columns in monkey striate cortex. *J. Neurosci.* 1993: 13: 4114–4129 doi: 10.1523/JNEUROSCI.13-10-04114.1993

Okamoto H, Ichikawa K. A model for molecular mechanisms of synaptic competition for a finite resource. *Biosystems* 2000: 55: 65 -71 doi:10.1016/S0303-2647(99)00084-2

Palacios ER, Razi A, Parr T, Kirchoff M, Friston K. On Markov blankets and hierarchical self-organisation. *Journal of Theoretical Biology* 2020: 486: 110089. doi.org/10.1016/j.jtbi.2019.110089

Parr T, Pezzulo G, Friston KJ. (2022) Active inference: the free energy principle in mind brain and behaviour. MIT Press. doi.org/10.7551/mitpress/12441.001.0001

Pavlos GP, Karakatsanis LP, Xenakis MN. Tsallis non-extensive statistics, intermittent turbulence, SOC and chaos in the solar plasma, Part one: Sunspot dynamics. Physica A. 2012: 391, 6287-6319. doi: 10.1016/j.physa.2012.07.066

Pearl J. (2009). Causality. Cambridge University Press, Cambridge. doi.org/10.1017/cbo9780511803161

Perin R, Berger TK, Markram H. A synaptic organizing principle for cortical neuronal groups. *Proc Natl Acad Sci USA* 2011: 108: 5419-5424. doi:10.1073/pnas.1016051108

Puelles L, Alonso A, Garcia-Calero E, Martinez-de-la-Torre M. Concentric ring topology of mammalian cortical sectors and relevance for patterning studies. *J Comp Neurol* 2019: 527: 1731-1752. doi:10.1002/cne.24650

Puelles L, Alonso A, Garcia-Calero E. Genoarchitectural Definition of the Adult Mouse Mesocortical Ring: A Contribution to Cortical Ring Theory. *J Comp Neurol* 2024: 532 (7): e25647. doi:10.1002/cne.25647

Pyragas K. Conditional Lyapunov exponents from time series. Physical Review E 1997: 56, 5183-5188. doi.org/10.1103/PhysRevE.56.5183

Rakic P. Neurogenesis in adult primate neocortex: an evaluation of the evidence. *Nat Rev Neurosci* 2002: 3: 65-71. doi:10.1038/nrn700

Ramstead MJD, Sakthivadivel DAR, Heins C, Koudahl M, Millidge B, Da Costa L, Klein B, Friston KJ. On Bayesian Mechanics: A Physics of and by Beliefs. *Interf. Focus*. 2022: 13: 20220029. doi: 10.1098/rsfs.2022.0029

Rennie CJ, Robinson PA, Wright JJ. Unified neurophysical model of EEG spectra and evoked potentials. *Biological Cybernetics* 2002: 86 457-471 doi:10.1007/s00422-002-0310-9

Rennie CJ, Wright JJ, Robinson PA. Mechanisms of cortical electrical activity and emergence of gamma rhythm. *Journal of Theoretical Biology* 2000: 05: 17-35 doi:10.1006/jtbi.2000.2040

Robinson PA, Rennie, CJ, Wright JJ. Propagation and stability of waves of electrical activity in the cerebral cortex. *Physical Review E* 1997: 56 826 doi:10.1103/PhysRevE.56.826

Robinson PA, Rennie CJ, Wright JJ, Bahramali H, Gordon E, Rowe DL. Prediction of electroencephalographic spectra from neurophysiology. *Physical Review E* 2001: 63 021930 doi:10.1103/PhysRevE.63.021903

Rockland KS, Lund JS. Intrinsic laminar lattice connections in primate visual cortex. *J Comp Neurol* 1983: 216: 303-318. doi:10.1002/cne.902160307

Sancha-Velasco A, Uceda-Heras A, Garcia-Cabezas MA. Cortical type: a conceptual tool for meaningful biological interpretation of high-throughput gene expression data in the human cerebral cortex. *Front Neuroanat* 2023: 17: 1187280. doi:10.3389/fnana.2023.1187280

Sang IEWF, Schroer J, Halbhuber L, Warm D, Yang J-W, Luhmann HJ, Kilb W, Sinning A. Optogenetically controlled activity pattern determines survival rate of developing neocortical neurons. *Int. J. Mol. Sci*. 2021: 22: 6575. doi: 10.3390/ijms22126575

Sanides F (1970) Functional architecture of motor and sensory cortices in primates in the light of a new concept of neocortex evolution. In: Noback CR, Montagna W (eds) The Primate Brain: Advances in Primatology. Appleton-Century-Crofts Educational Division/Meredith Corporation, New York (NY), pp 137-208

Sanides F. Architectonics of the human frontal lobe of the brain. With a demonstration of the principles of its formation as a reflection of phylogenetic differentiation of the cerebral cortex]. *Monogr Gesamtgeb Neurol Psychiatr* 1962: 98: 1-201. PMID: 13976313

Sanides F. The cyto-myeloarchitecture of the human frontal lobe and its relation to phylogenetic differentiation of the cerebral cortex. *J. Hirnforsch* 1964: 47: 269-282 PMID 14227452

Schiff SJ, So P, Chang T, Burke RE, Sauer T. Detecting dynamical interdependence and generalized synchrony through mutual prediction in a neural ensemble. Physical Review E 1996: 54, 6708-6724. doi.org/10.1103/PhysRevE.54.6708

Schumacher J, Haslinger R, Pipa G, 2012. Statistical modeling approach for detecting generalized synchronization. Physical Review E. 2012: 85, 056215. doi.org/10.1103/PhysRevE.85.056215

Sengupta B, Stemmler MB, Friston KJ. Information and efficiency in the nervous system--a synthesis. PLoS Comput Biol 2013: 9, e1003157. doi.org/10.1371/journal.pcbi.1003157

Shipp S, Friston K. (2022) Predictive coding: forward and backward connectivity. In: W. Martin Usrey and S Murray Sherman (eds). The Cerebral Cortex and the Thalamus (pp 436-445). Oxford Academic. doi.org/10.1093/med/9780197676158.003.ppi

Singer W. (1993) Synchronization of cortical activity and its putative role in information processing and learning. *Annual Review of Physiology* 1993: 55: 349-374 doi:10.1146/annurev.ph.55.030193.002025

Sperry RW. Some effects of disconnecting the cerebral hemispheres. *Nobel Prize Lecture.* 1981.

Trevarthan CB. Two mechanisms of vision in primates. *Psychological Research* 1968: 31: 299-337 link.springer.com/article/10.1007/BF00422717

Tsuda I. Toward an interpretation of dynamic neural activity in terms of chaotic dynamical systems. Behavioral and Brain Sciences 2001: 24, 793-748. doi:10.1017/s0140525x01000097

Tucker DM, Luu P. Motive control of unconscious inference: the limbic basis of adaptive Bayes. *Neuroscience and Biobehavioural Reviews.* 2021: 128: 328-345. doi.org/10.1016/j.neurobiorev.2021.06.029

Tucker DM, Luu P, Friston KJ .The criticality of consciousness: excitatory-inhibitory balance and dual memory systems in active inference*. Entropy* 2025 27:829 doi.org/10.3390/e27080829

Tucker DM, Luu, P. Adaptive control of functional connectivity: dorsal and ventral limbic divisions regulate the dorsal and ventral neocortical networks. *Cerebral Cortex* 2023: 33: 7870-7895 doi: 10.1093/cercor/bhad085.

Tucker DM, Luu P. Excitatory-inhibitory resonance in cognition stabilizes synaptic traces in memory. *Cerebral Cortex* 2026 (in press)

Thye M, Ding J, Hoffman P, Mirman D. Functional connectivity of semantic and default networks during narrative comprehension. *Cerebral Cortex* 2025 35:bhaf289 doi.org/10.1093/cercor/bhaf289

Ungerleider LG, Mishkin M. (1982). Two cortical visual streams. In D.J. Ingle, M.A. Goodale & R.J.W. Mansfield (Eds.) Analysis of Visual Behavior (pp. 549–586). Cambridge, MA: MIT Press. https://irp.nih.gov/accomplishments/anatomy-of-perception-identifying-two-visual-streams-in-the-brain.

Vezoli J, Magrou L, Goebel R, Wang X-J, Knoblauch K, Vinck M, Kennedy H. Cortical hierarchy, dual counterstream architecture and the importance of top-down generative networks. *Neuroimage* 2021: 225: 117479 doi:10.1016/j.neuroimage.2020.117479

Vidyasagar TR, Eysel UT. Origins of feature selectivities and maps in the mammalian primary visual cortex. *Trends Neurosci.* 2015: 38: 475–485. doi.org/10.1016/jtins.2015.06.003

Wandell BA, Dumoulin SO, Brewer AA. Visual maps in human cortex. *Neuron* 2007 56:366-383 doi.org/10.1016/j.neuron.2007.10.012

Wiesel TN, Hubel DH. Ordered arrangement of orientation columns in monkeys lacking visual experience. *J. Comput. Neurol.* 1974: 158: 307–318. doi: 10.1002/cne.901580306

Wright JJ, Bourke PD, Chapman CL. Synchronous oscillation in the cerebral cortex and object coherence: simulation of basic electrophysiological findings. *Biological Cybernetics* 2000: 83: 341-353. doi:10.1007/s004220000155

Wright JJ, Bourke PD, Favorov OV. Mobius-strip-like columnar functional connections are revealed in somato-sensory receptive field centroids. *Front. Neuroanat.* 2014: 8. doi.org/10.3389/fnana.2014.00119

Wright JJ, Bourke PD. Further work on the shaping of cortical development and function by synchrony and metabolic competition. *Front. Comp. Neurosci.* 2016:10. doi:10.3389/fncom.2016.00127

Wright JJ, Bourke PD. Markov blankets and mirror symmetries – free energy minimization and mesocortical anatomy. *Entropy* 2024a: 26: 287. doi.org/10.3390/e26040287

Wright JJ, Bourke PD. Cortical development in the structural model and free energy minimization. Cerebral Cortex 2024b: 34:bhae416 doi.org/10.1093/cercor/bhae416

Wright JJ, Bourke PD. Minimization of prediction error during cerebral embryogenesis and the emergence of agency. *Frontiers in Systems Neuroscience* 2025: 19: doi.org/10.3389/fnsys.2025.1683448

Wright JJ, Bourke PD. On the dynamics of cortical development: synchrony and synaptic self-organization. *Front. Comp. Neurosci.* 2013: 7. doi:10.3389/fncom.2013.00004

Wright JJ, Bourke PD. Unification of free energy minimization, spatio-temporal energy, and dimension reduction models of V1 organization:postnatal learning on an antenatal scaffold. *Front. Comput. Neurosci.* 2022: 16. doi:10.3389/fncom.2022.869268

Wright JJ, Liley DTJ. Simulation of electrocortical waves. *Biological Cybernetics* 1995: 72: 347-356 doi;10.1007/BF00202790

Wright JJ, Liley DTJ. Dynamics of the brain at global and microscopic scales: neural networks and the EEG. *Behavioral and Brain Sciences* 1996: 19:285-295 doi.org 10.1017/s0140525x00042679

Yang F-C, Dokovna LB, Burwell RD. Functional differentiation of dorsal and ventral posterior parietal cortex of the rat: implications for controlled and stimulus-driven attention. *Cerebral Cortex* 2022: 32: 1787-1803 doi:10.1093/cercor/bhab308

Yeo BTT, Krienen FM, Sepulcre J, Sabuncu MR, Lashkari D, Hollinshead M, Roffman JL, Smoller JW, Zollei L, Polimeni JR, Fischi B, Liu H, Buckner RL (2011). The organization of the human cerebral cortex estimated by intrinsic functional connectivity. *J. Neurophysiol. 2011:* 106, 1125–1165. doi: 10.1152/jn.003 38.2011

Yuan R, Ma Y, Yuan B, Ping A. Bridging Engineering and Physics: Lyapunov Function as Potential Function. arXiv:1012.2721v1 2010. doi.org/10.1088/1674-1056/23/1/010505

Zeki S, Shipp S. The functional logic of cortical connections. Nature 1988: 335, 311-317. doi:10.1038/335311a0

Zhang JX, Rosenberg A, Mallik AK, Husson TR, Issa NP. The representation of complex images in spatial frequency domains of primary visual cortex. *J. Neurosci.* 2007: 279310–9318. doi: 10.1523/JNEUROSCI.0500-07.2007.